September Arctic Sea Ice minimum prediction – a new skillful statistical approach

Monica Ionita[1,2], Klaus Grosfeld[1], Patrick Scholz[1], Renate Treffeisen[1], Gerrit Lohmann[1,2]

[1] Alfred Wegener Institute Helmholtz Center for Polar and Marine Research, Bremerhaven, 27570, Germany

5   [2] MARUM – Center for Marine Environmental Sciences, University of Bremen, Bremen, Germany

Correspondence to: Monica Ionita (Monica.Ionita@awi.de)

Abstract. Sea ice in both Polar Regions is an important indicator for the expression of global climate change and its polar amplification. Consequently, a broad interest exists on sea ice coverage, variability and long term change. However, its predictability is complex and it depends strongly on different atmospheric and oceanic
10 parameters. In order to provide insights into the potential development of a monthly/seasonal signal of sea ice evolution, we applied a robust statistical model based on different oceanic and atmospheric parameters to calculate an estimate of the September sea ice extent (SSIE) on monthly time scale. Although previous statistical attempts of monthly/seasonal SSIE forecasts show a relatively reduced skill, when the trend is removed, we show here that the September sea ice extent has a high predictive skill, up to 4 months ahead, based on previous
15 months' oceanic and atmospheric conditions. Our statistical model skillfully captures the interannual variability of the SSIE and could provide a valuable tool for identifying relevant regions and oceanic and atmospheric parameters that are important for the sea ice development in the Arctic and for detecting sensitive/critical regions in global coupled climate models with focus on sea ice formation.

20 ## 1 Introduction

Arctic sea ice plays an important role in modulating the global climate system by influencing the atmospheric and oceanic circulation in Polar Regions. Moreover, it has a strong impact also on the global economic system through changes in marine and natural resources development. The sea ice extent and thickness over the Arctic region has undergone an extraordinary decline during the last decades that can be linked to climate change
25 (Allison et al., 2009; Kay et al., 2011; Notz and Marotzke, 2012). The trends in the Arctic sea-ice extent are negative for all months, with the largest trend recorded at the end of the melt season in September (Serreze et al., 2007), with an average decline of 12.9% per decade relative to the long-term mean of 1981-2010 September average (Grosfeld et al., 2016). These negative trends, with their environmental and economic implications as well as its impacts on human society, have led to a rising demand for accurate sea ice predictions at monthly,

seasonal up to decadal time scales, which in turn will be able to address the growing demands from different stakeholders and the scientific community (Meier et al., 2014). As such, an accurate sea ice prediction plays a crucial role for ecosystems, coastal communities, planning for new shipping ports, oil and gas exploration and marine transportation. For example, the exploitation of shipping via the Northwest Passage or Northeast Passage

5   could reduce the navigational distance between Europe and Asia by ~40% when compared to the route via the Suez canal (Schøyen and Bråthen, 2011). Overall, the summertime use of these routes by different vessels (i.e. cargo ship and tanks) has increased (Eguíluz et al., 2016), thus the need for a proper forecast for the Arctic sea ice conditions has become imperative. As such, an early knowledge on the potential opening of the maritime Arctic routes could allow a better management for the shipping companies to optimize (in terms of time and costs)

10   shipping routes between the Atlantic and the Pacific Oceans (Hassol, 2004; Smith and Stephenson, 2013). However, the opening of the Northeast and Northwest Passages does not guarantee ice free transects along the passages at all times and can always include the possibility of drifting ice flows, which for conventional ships poses high risks and potential environmental danger when getting damaged in case of accidents. Hence, a proper forecast does not imply a dangerous free transect as long as the Arctic Ocean is ice covered with thick multiyear

15   ice for its larger parts over the significant times of the year.

Although the evolution of Arctic sea ice physical properties has been extensively studied, the prediction of detrended Arctic sea ice extent, with lead times of 3 months and longer, have not been very promising (Lindsay et al., 2008; Blanchard- Wrigglesworth et al., 2011). Currently, there are different approaches used to make sea ice forecast: ice-ocean-atmosphere coupled models, statistical models, best guesses model and mixed models

20   (Stroeve et al., 2014; Hamilton and Stroeve, 2016). From a statistical point of view, Drobot et al. (2006) showed that 46% of the pan-Arctic minimum sea ice extent would be predictable as early as February based on monthly sea ice concentration, surface albedo, downwelling long-wave radiation and surface skin temperature. Lindsay et al. (2008) have shown that their statistical model based on a wide range of predictors (e.g., atmospheric circulation indices, sea ice extent and sea ice concentration, ocean temperature at different levels) exhibited a

25   greater skill in predicting the September sea ice extent (SSIE) than those by Drobot et al. (2006). The forecasts based on the state-of-the-art coupled atmosphere-ocean sea ice models (Chevallier et al., 2013; Sigmond et al., 2013) do not show better results when compared with the statistical models (Kapsch et al., 2014; Schröder et al., 2014; Zhan and Davies, 2017). These caveats indicate that our understanding regarding the controlling factors of Arctic sea ice may still be insufficient. Overall, skilful forecasts extend only 2 to 5 months ahead, for the summer

30   months (Stroeve et al., 2015; Schröder et al., 2014), regardless of the type of the model used for the forecast (dynamical or statistical). The results and error margins based on these different approaches have highlighted

how difficult it is to make skillful prediction for the SSIE, especially for the years with extreme low September sea ice concentrations (e.g., 2012 or 2007), with both, the dynamical and the statistical models showing similar limitations (Stroeve et al., 2015; Schröder et al., 2014; Stroeve et al., 2014; Hamilton and Stroeve, 2016). Stroeve et al. (2014) have shown that seasonal predictions of the SSIE are most accurate in years when the sea ice extent

5   is near the long-term trend, but skillful sea ice extent prediction appear challenging in years when the weather plays a larger role (Hamilton and Stroeve, 2016).

In order to improve the monthly/seasonal prediction skill of the sea ice extent one possibility would be to identify stable predictors (the correlation coefficient between the predictor and the predictand does not change in time) and to develop a statistical forecast model based on these predictors. Following this idea, here we analyze the

10 oceanic and atmospheric conditions associated to the SSIE in order to identify potential predictors based on a simple statistical methodology and placed them in a longer temporal context. Our statistical model takes into account different atmospheric and oceanic variables: sea level pressure (SLP), air temperature (TT), precipitable water content (PWC), surface zonal wind (USURF), surface meridional wind (VSURF), the ocean heat content integrated over the first 700m (OHC), sea surface temperature (SST) and water temperature integrated over the

15 first 100m (OT100), in order to calculate an estimate of SSIE. The paper is structured as follows: the data and methods used in this study are presented in Section 2, while the main results of our analysis are shown in Section 3. The concluding remarks are presented in Section 4.

2 Data and methods

20 ### 2.1 Data

The sea ice concentration has been extracted from the National Snow and Ice Data Center (NSIDC) database. The sea ice concentration (SIC) is processed using the NSIDC bootstrap algorithm (Comiso and Nishio, 2008; Meier et al., 2013). The sea ice extent (SIE) is defined as the total area of all satellite pixels where the sea ice concentration equals or exceeds 15%. The monthly sea ice extent index (Fetterer et al., 2016) has been extracted

25 from the NSIDC ftp server (ftp://sidads.colorado.edu/DATASETS/NOAA/G02135/north/).

For the Northern Hemisphere temperature and atmospheric circulation, we use the monthly means of air temperature at 2m (TT), downward longwave radiation flux (DW), zonal wind (USURF), meridional wind (VSURF), precipitable water content (PWC) and the mean sea level pressure (SLP) from the NCEP/NCAR 40-year reanalysis project (Kalnay et al., 1996) on a 2.5° x 2.5° grid. Global sea surface temperature (SST) is

30 extracted from the Extended Reconstructed Sea Surface Temperature data (ERSSTv4b) (Huang et al., 2014). This

dataset covers the period 1854 – present and has a spatial resolution of 2° x 2°. The global heat content data in the first 700m (OHC) and the ocean temperature integrated over the first 100m (OT100) is extracted from the Global Ocean Heat and Salt Content database (Levitus et al., 2012; Boyer et al., 2013).

2.2 Stability Maps

The statistical model used in this study for the estimation of SSIE is based on a methodology successfully used to make monthly/seasonal streamflow predictions for the central European rivers (e.g. Elbe river, Rhine river, Danube river), as well as for identifying the drivers of the Antarctic sea ice variability (Ionita et al., 2008, 2014, 2017, 2018; Meißner et al., 2017). The basic idea of this procedure is to identify regions with stable teleconnections between the predictors and the predictand. The SSIE has been correlated with the potential predictors from previous months (years), in a moving window of 21 years and the statistical significance of the correlation coefficient was tested using a *Student* t-test. The correlation is considered *stable* for those grid-points where SSIE and the large-scale predictors (e.g. OHC, OT100, SST, SLP, TT, PWC, DW, USURF and VSURF) are significantly correlated at 95%, 90%, 85% and 80% level for more than 80% of the 21-year windows, covering the period 1979-2007. The area where the correlation coefficient is stable and positive are represented as dark red (95%), red (90%), orange (85%) and yellow (80%), while the regions where correlation coefficient is stable and negative are represented as dark blue (95%), blue (90%), green (85%) and light green (80%). Such maps are referred in our study as *stability maps* and their spatial structures remain qualitatively the same if the significance levels that define the stability of the correlation vary within reasonable limits and if the length of the moving window varies between 15 to 25 years. For the current analysis only regions where the correlation is above 90% significance level, are retained for further analysis. All the data sets have been detrended before the analysis.

2.3 Multiple Linear Regression

For the forecast m all datasets were separated into two parts: 1) the calibration period (1979–2007) and 2) the validation period (2008 – 2017). The optimal predictors are identified by employing stepwise multiple regression analysis. Although the "stable maps" methodology identifies multiple stable regions for each atmospheric/oceanic parameters, after applying the stepwise multiple regression, the optimal/final prediction model is based just on the most significant regions.

To forecast the September Sea Ice Extent we have used a multiple linear regression model with the regression equation:

$$Y = \beta_0 + \beta_1 x_1 + \beta_2 x_2 + \cdots + \beta_n x_n + \varepsilon$$

where Y represents the SSIE index, $\beta_o, \beta_1, \beta_2, \ldots \beta_n$ are constants determined by the least squares procedure, $x_1, x_2, \ldots x_n$ the predictors used (e.g., OHC, OT100, etc) and ε the error.

In this study we choose stepwise regression because it prioritizes predictors based on the partial correlation and it is likely that high and significant correlations will reflect underlying physical processes.

3 Results

3.1 Pan-Arctic September sea ice prediction

The skill of a long-range forecast for the Arctic SSIE is associated with the predictors that represent the slow varying components of the climate system that are able to integrate the climate information such as sea ice, snow cover, ocean heat content and SST (Guemas et al., 2014, Lindsay et al., 2008). These variables can be used as potential predictors for months and even seasons in advance due to their long-term memory. Thus, here we investigate the potential link between the Arctic SSIE (Fetterer et al., 2016) and OHC, OT100 (Levitus et al., 2012; Boyer et al., 2013) and SST (Huang et al., 2014) as long-term predictors (lags ~4 years up to 4 months in advance). On shorter time-scales (2 – 4 months) the atmospheric circulation, especially during the summer months, plays a major role in driving the Arctic sea ice variability (Guemas et al., 2014). The atmospheric circulation, if predictable, can substantial contribute to the skill of the sea ice predictions. As such, for the SSIE prediction we have also tested the skill of atmospheric variables (up to 4 months in advance), e.g., SLP, TT, PWC, USURF and VSURF (Kalnay et al., 1996). Sea level pressure is seen as an estimate of the general atmospheric circulation pattern, while USURF and VSURF fields are treated as advective parameters (Guemas et al., 2014). As an additional predictor we have used PWC, which can give an indication of the water vapor content in the atmosphere, which in turn affects the SSIE via the greenhouse effect (Kapsch et al, 2013). Increased cloudiness and humidity also lead to an enhanced greenhouse effect, which again enhances sea ice melt, especially during the spring months (Kapsch et al., 2013; Kapsch et al., 2014).

As a further main contributor to our forecast model, we use persistence, defined here as the sea ice extent from previous months (e.g., January, February up to August). Persistence of sea ice anomalies stands as the first source of predictability for sea ice (Guemas et al., 2014; Walsh et al., 1979; Blanchard-Wrigglesworth et al., 2011). In order to identify possible stable relationships between these identified predictors and the SSIE, the stability

correlation maps (see Methods for definition) are calculated between the SSIE index on the one hand and the gridded fields of the above mentioned atmospheric/oceanic variables on the other hand, with different lags, depending on the variable. The optimal predictors are defined as the average values over the stable regions for each gridded parameter.

5   For the final forecast, based on data available at the end of May (4 months ahead forecast) we have retained all the stable regions (black boxes in Figure 1) for all variables based on previous month's data. For the forecast based on June data, we have included also the stable regions based on all June stability maps (Figure 2). We have applied the same technique for the July data (Figure 3). For SSIE prediction based on the end of May data, the optimal model is based on a combination of: OHC SON, SST MAM, PWC Apr, VSURF MAM and SLP May

10   (*Table 1*). Together with these identified stable regions, the optimal model includes also the persistence of sea ice extent (here the sea ice extent index from previous March (SIE Mar), as well as the annual Atlantic Multidecadal Oscillation index, with a lag 4 of years (AMO L4). Overimposed on the interannual variability, the temperature and salinity of the Atlantic inflows to the Arctic Ocean shows also pronounced decadal to multidecadal variability (Zhang, 2015). This aligns with the concept of different previous studies, which suggest that the

15   decreasing trend in the Artic sea ice is partially driven by AMO (Park and Latif, 2008; Lindsay et al., 2005; Ding et al., 2014; Yu et al., 2017). In a recent study, Yu et al., (2017) have shown that two thirds of the total global sea ice trend can be explained by a combination of AMO and Pacific Decadal Oscillation (PDO). Moreover, starting at the beginning of 1990's the AMO has switched to a positive phase, at the same time when the Artic sea ice extent started its abrupt decline. Thus, in this study we have tested previous years AMO index as a potential

20   driver of the Arctic sea ice extent. The highest correlation between SSIE and the annual AMO index was found at a time lag of 4 years (AMO leads SSIE). The time lag identified in our analysis is in line with previous studies (Day et al., 2012; Mahajan et al., 2011). The observed and forecasted values based on the May data are shown in Figure 4a. The explained variance of the model, over the calibration (*validation*) period, is 81% (*71%*) and the correlation coefficient between the observed and forecasted SSIE is r = 0.90 (*r = 84*) (99.9% significance level).

25   To better assess the skill of the SSIE prediction, the root mean square error (RMSE), the Nush-Sutcliffe efficiency (NSE) and the index of agreement (d) are calculated, among other statistical tests (see Table S1 and supplementary file for a definition of all the metrics used to test the skill of the model). The forecasted model based on May data shows a very good skill (Table S1) NSE = 0.82 (*0.68*) (NSE = 1 means perfect model) and d = 0.95 (*0.88*) (d = 1 indicates a perfect match between the observed and forecasted values, d = 0 indicates no

30   agreement at all).

Following the same steps as in the case of May data, for the model based on June data, the parameters contributing to the optimal forecast model are shown in Figure 2. As additional predictors we have: VSURF Jun, USURF Jun and TT Jun (*Table 1*). The observed and forecasted values of SSIE based on June data are shown in Figure 4b. The overall explained variance of the June-based model, over the calibration (*validation*) period, is

5   85% (*79%*) and the correlation coefficient between the observed and forecasted SSIE values is r = 0.92 (*r = 0.89*) (99.9% significance level). The June-based model exhibits also a very good skill and shows slight improvements compared to the May – based model (NSE = 0.85 (*0.78*) and d = 0.96 (*0.93*). For the model based on July data, the parameters contributing to the optimal forecast model are shown in Figure 3 and Table 1. The observed and predicted values of SSIE based on July data are shown in Figure 4c. The overall explained variance of the June-

10   based model, over the calibration (*validation*) period, is 86% (*81%*) and the correlation coefficient between the observed and forecasted SSIE values is r = 0.93 (*r = 0.90*) (99.9% significance level). The July-based model exhibits also a very good skill and shows also slight improvements compared to the May and June – based models (NSE = 0.86 (*0.80*) and d = 0.96 (*0.94*)).

3.2 Robustness of the methodology

15   To test the robustness of our statistical model and to move towards stakeholder-relevant regions, in this study we are investigating also the skill of our model at regional scale. Thus, we have repeated the same analysis as in the previous section but for the sea ice extent averaged over the East Siberian Sea (ESS) (Figure S1). In this study we focus on the ESS due to the fact that in September 2007 and 2012, negative ice concentration anomalies were particularly pronounced over East Siberian Sea sector of the Arctic Ocean (Figure S1a and S1b, respectively) and

20   the highest variability of the SSIE is recorded over this region (Figure S1c). Overimposed on this, since 2011 the eastern ESS has been nearly ice free (<10%) at the end of summer (Polyakov et al., 2017). Moreover, when looking at the correlation coefficients between the pan-Arctic SSIE and regional September SIE, the highest correlation, at lag 0, is found with the EES sea ice extent (r = 0.72, Table 2). At seasonal time scale, for the Laptev Sea and ESS, a high predictive skill was found for the sea ice thickness, mainly due to persistence, while

25   for the sea ice concentration the prediction skill is very low (Koenigk and Mikolajewicz, 2009).

The stability maps between the detrended ESS September sea ice extent and the large scale oceanic and atmospheric fields are shown in Figure S2 (stability maps based on May and previous months data), Figure S3 (stability maps based on June and previous months data) and Figure S4 (stability maps based on July and previous months data), respectively. For ESS SSIE prediction based on the end of May data, the optimal model is

30   based on a combination of: annual OT100, SST MAM, SLP Jan, VSURF MAM, PWC May, TT May and DW

MAM (*Table 3*). The observed and forecasted values based on the May data are shown in Figure 5a. The explained variance of the model, over the calibration (*validation*) period, is 88% (*58%*) and the correlation coefficient between the observed and forecasted ESS SSIE is r = 0.94 (*r = 77*) (99.9% significance level). The forecasted model based on the May shows a very good skill (Table S2) NSE = 0.88 (*0.57*) (NSE = 1 means perfect model) and d = 0.97 (*0.86*) (d = 1 indicates a perfect match between the observed and forecasted values, d = 0 indicates no agreement at all).

For the model based on June data, the parameters contributing to the optimal forecast model are shown in Figure S3 and Table 3. As additional predictors, compared to end of May data, we have: SIE Jun, and TT Jun (*Table 3*). The observed and forecasted values of ESS SSIE based on June data are shown in Figure 5b. The overall explained variance of the June-based model, over the calibration (*validation*) period, is 91% (*71%*) and the correlation coefficient between the observed and forecasted SSIE values is r = 0.95 (*r = 0.84*) (99.9% significance level). The June-based model exhibits also a very good skill and shows slight improvements compared to the May – based model (NSE = 0.91 (*0.69*) and d = 0.98 (*0.91*). For the model based on July data, the parameters contributing to the optimal forecast model are shown in Figure S4 and Table 3. The observed and predicted values of SSIE based on July data are shown in Figure 5c. The overall explained variance of the July-based model, over the calibration (*validation*) period, is 94% (*81%*) and the correlation coefficient between the observed and forecasted SSIE values is r = 0.97 (*r = 0.90*) (99.9% significance level). The July-based model exhibits also a very good skill and shows also slight improvements compared to the May and June – based models (NSE = 0.94 (*0.78*) and d = 0.98 (*0.93*)).

4 Conclusions

The results of this study demonstrate that statistically based models are able to skillfully predict SSIE, if the accurate drivers and their regional localizations (stable regions) are identified via various statistical techniques. Although our analysis was focused on a single month - September, a similar statistical model will be applied also for other months/seasons and also for the Antarctic region. Overall, such a methodology can be valuable also for the modelling community. If the coupled models, used for forecasting purposes, face problems to simulate the ocean and/or the climate background over the areas that play a significant role in driving the SSIE variability (stable regions), one expects a relatively small skill in their forecast. The opposite case is also valid: a good representation of the key regions that drive SSIE could imply a good forecast skill. For example, Parkinson et al. (2006) determined that many climate models tend to simulate more winter sea ice in the Barents Sea compared to observations. One hypothesis for this overestimation is that the models underestimate the heat content in the

Atlantic Basin (which has proved to be one of the main contributors for a skillful prediction for SSIE in our model).

Our results highlight the potential for skillful prediction of SSIE, both at pan-Arctic level as well as for EES, based on ocean and climate variables from stable regions. The ocean drivers (OHC, TT100 and SST) from the identified stable regions are strongly related with the Atlantic inflow (the stable regions over the western European coast) or with the SST variability over regions strongly influenced by decadal modes of variability (e.g., Pacific Decadal Oscillation (PDO) in the central and north Pacific) to multidecadal modes of variability (e.g., Atlantic Multidecadal Oscillation (AMO) in the Atlantic Ocean region). The Atlantic inflow, AMO and PDO play a significant role in driving the Arctic sea ice variability (Polyakov et al., 2017; Miles et al., 2014; Ionita et al., 2016; Screen et al., 2016). For example, the North Atlantic might act as a source for the OHC anomaly identified over the Kara Sea, Laptev Sea and EES (Figure 1a), thus contributing to the skill of our forecast. The OHC anomalies form the North Atlantic flow into the Arctic basin, via advection, affect the sea ice distribution (Polyakov et al., 2017, Ono et al., 2018). In a recent study, Yu et al., (2017) have shown that the leading mode of variability of global sea-ice concentration is positively correlated with the AMO and negatively correlated with the PDO and two thirds of the total global sea ice trend can be explained by a combination of these two modes of variability. The stability maps based on the predictors related to the atmospheric variables (e.g., SLP, PWC, TT and so on) show significant and stable correlations with regions restricted to the Artic basin, indicating a much regional connection between the September sea ice variability and large-scale atmospheric circulation. The state of the Arctic SSIE depends both on the state of the ice in spring as well as on the atmospheric condition during summer (Ding et al., 2017). In this respect, the precipitable water content and air temperature in spring and early summer were found to show significant predictive skill for the SSIE both at pan-Arctic as well as regional level. This is also in agreement with previous studies (Kapsch et al., 2014; 2015) which have shown that a significantly enhanced transport of humid air during spring produces increased cloudiness and humidity, thus accelerating the sea ice retreat in the upcoming summer.

By using a simple and computationally inexpensive statistical approach, one can anticipate more than 80% of SSIE up to 4 months in advance, based on the antecedent atmospheric and oceanic conditions over stable regions. Moreover, our statistical model is able to properly reproduce the years with extreme low / high sea ice extent, both at pan-Arctic level as well as at regional scale (e.g., 2007 and 2012 – low SSIE and 1996 – high SSIE; see Figure 4 and Figure 5). The predictability of these extreme years poses big challenges for the sea ice prediction community (Hamilton and Stroeve, 2016). We argue that our statistical approach can be used as a promising tool to improve the skill of sea ice extent prediction. The same methodology will be applied in the future to test the

potential predictability, up to 2 years ahead, by taking into account variables with long-term memory (e.g., heat content and water temperature integrated over different depths) for the whole Arctic, for other regions prone to extreme decrease in the sea ice extent (e.g., Chukchi Sea, Beaufort Sea, Barents Sea) as well as for Antarctica . Finally, since the concept can be used as an early warning system for September sea ice extent, both at pan-Arctic

5   level as well as regionally, the potential environmental and economic benefits can be very high.

25

30

Acknowledgements. This study is promoted by Helmholtz funding through the Polar Regions and Coasts in the Changing Earth System (PACES) program of the AWI. Funding by the Helmholtz Climate Initiative REKLIM is gratefully acknowledged. P. Scholz has been funded by the Collaborative Research Centre TRR 181 "Energy Transfer in Atmosphere and Ocean".

25

30

References

Allison, I., Bindoff, N.L., Bindschadler, R.A., Cox, P.M., de Noblet, N., England, M.H., Francis, J.E., Gruber, N., Haywood, A.M., Karoly, D.J., Kaser, G., Le Quéré, C., Lenton, T.M., Mann, M.E., McNeil, B.I., Pitman, A.J., Rahmstorf, S., Rignot, E., Schellnhuber, H.J., Schneider, S.H., Sherwood, S.C., Somerville, R.C.J., Steffen, K., Steig, E.J., Visbeck, M., and Weaver, A.J. The Copenhagen Diagnosis: Updating the World on the Latest Climate Science. Sydney, Australia: University of New South Wales, Climate Change Research Centre. Available at http://www.ccrc.unsw.edu.au/Copenhagen/Copenhagen_Diagnosis_LOW.pdf, 2009.

Blanchard-Wrigglesworth, E., Armour, K.C., Bitz, C.M., and DeWeaver, E. Persistence and inherent predictability of Arctic sea ice in a GCM ensemble and observations. J. Clim. 24: 231–250, 2011.

Boyer, T.P., Antonov, J. I., Baranova, O.K., Coleman, C., Garcia, H.E., Grodsky, A., Johnson, D.R., Locarnini, R.A., Mishonov, A.V., O'Brien, T.D., Paver, C.R., Reagan, J.R., Seidov, D., Smolyar, I.V., and Zweng, M.M. World Ocean Database 2013, NOAA Atlas NESDIS 72, S. Levitus, Ed., A. Mishonov, Technical Ed.; Silver Spring, MD, 209 pp., 2013.

Cavalieri, D.J., Parkinson, C.L., Gloersen, P., and Zwally, H.J. Arctic and Antarctic Sea Ice Concentrations from Multichannel Passive-Microwave Satellite Data Sets: October 1978-September 1995 - User's Guide - *NASA TM 104647.* Goddard Space Flight Center, Greenbelt, MD 20771, pp1, 1997.

Comiso, J. C.*, and Nishio, F. Trends in the sea ice cover using enhanced and compatible AMSR-E, SSM/I, and SMMR data, J. Geophys. Res.*, 113*, C02S07, doi:*10.1029/2007JC004257, 2008.

Day, J.J., Hargreaves, J.C., Annan, J.D., and Abe-Ouchi, A. Sources of multi-decadal variability in Arctic sea ice extent, *Environ. Res. Lett.*, 7, 034011, doi:10.1088/1748-9326/7/3/034011, 2012.

Ding, Q., Schweiger, A., L'Heureux, M., Battisti, D.S., Po-Chedley, S., Johnson, N.C., Blanchard-Wrigglesworth, E., Harnos, K., Zhang, Q., Eastman, R., and Steig, E.J. Influence of high-latitude atmospheric circulation changes on summertime Arctic sea ice, Nature Climate Change, doi:10.1038/nclimate3241, 2017.

Ding, Q., Wallace, J.M., Battisti, D.S., Steig, E.J., Gallant, A.J.E., Kim, H.-J., and Geng, L. Tropical forcing of the recent rapid Arctic warming in northeastern Canada and Greenland. Nature 509, 209–212, 2014.

Drobot, S.D., Maslanik, J.A., and Fowler, C. A long-range forecast of Arctic summer sea ice minimum extent. *Geophys. Res. Lett.* **33**: L10501, doi:10.1029/2006GL026216, 2006.

Eguíluz V. M., Fernández-Gracia, J., Irigoien ,X., and Duarte, C. M. A quantitative assessment of Arctic shipping in 2010–2014. Sci. Rep. 6, 30682, doi:10.1038/srep30682, 2016.

Fetterer, F., Knowles, K., Meier, W. and Savoie, M. Updated daily Sea Ice Index, Version 2. Boulder, Colorado USA. NSIDC: National Snow and Ice Data Center. doi: http://dx.doi.org/10.7265/N5736NV7, 2016.

Grosfeld, K., Treffeisen, R., Asseng, J., Bartsch, A., Bräuer, B., Fritzsch, B., Gerdes, R., Hendricks, S., Hiller, W., Heygster, G., Krumpen, T., Lemke, P., Melsheimer, C., Nicolaus, M., Ricker, R., and Weigelt, M. Online sea-ice knowledge and data platform, available at: http://www.meereisportal.de (last access: 6 August 2017), Alfred Wegener Institute for Polar and Marine Research & German Society of Polar Research, Bremerhaven, 85, 143–155, https://doi.org/10.2312/polfor.2016.011, 2016.

Guemas, V., Blanchard-Wrigglesworth, E., Chevallier, M., Day, J.J., Déqué, M., Doblas-Reyes, F.J., Fučkar, N.S., Germe, A., Hawkins, E., Keeley, S., Koenigk, T., Salas y Mélia, D., and Tietsche, S. A review on Arctic sea-ice predictability and prediction on seasonal to decadal time-scales. Q.J.R. Meteorol. Soc., 142: 546-561. doi:10.1002/qj.2401, 2016.

Hamilton, L., and Stroeve, J.C. 400 Predictions: the SEARCH Sea Ice Outlook 2008–2015. Polar Geography, 39:4, 274-287, 2016.

Hassol, S,J. Impacts of a Warming Arctic: Arctic Climate Impact Assessment. Cambridge University Press: Cambridge, UK. http://www.amap.no/arctic-climate-impact-assessment-acia, 2004.

Huang, B., Banzon, V.F., Freeman, E., Lawrimore, J., Liu, W., Peterson, T.C., Smith, T.M., Thorne, P.W., Woodruff, S.D., and Zhang, H.-M. Extended Reconstructed Sea Surface Temperature version 4 (ERSST.v4): Part I. Upgrades and intercomparisons. Journal of Climate, 28, 911–930, doi:10.1175/JCLI-D-14-00006.1, 2014.

Ionita, M., Dima, M., Lohmann, G., Scholz, P., and Rimbu, N. Predicting the June 2013 European Flooding based on Precipitation, Soil Moisture and Sea Level Pressure. J. Hydrometeorology, 16, 598–614., doi: http://dx.doi.org/10.1175/JHM-D-14-0156.1, 2014.

Ionita, M., Lohmann, G. and Rimbu, N. Prediction of Elbe discharge based on stable teleconnections with winter global temperature and precipitation, Journal of Climate, 21, 6215–6226, doi:10.1175/2008JCLI2248.1, 2008.

Ionita, M., Scholz, P., Lohmann, G., Dima, M. and Prange, M. Linkages between atmospheric blocking, sea ice export through Fram Strait and the Atlantic Meridional Overturning Circulation, Scientific Reports, 6: 32881, 2016.

Ionita, M., Scholz, P., Grosfeld, K., and Treffeisen, R.: Moisture transport and Antarctic sea ice: austral spring 2016 event, Earth Syst. Dynam., 9, 939-954, https://doi.org/10.5194/esd-9-939-2018, 2018.

Kalnay, E., Kanamitsu, M., Kistler, R., Collins, W., Deaven, D., Gandin, L., Iredell, M., Saha, S., White, G., Woollen, J., Zhu, Y., Chelliah, M., Ebisuzaki, W., Higgins, W., Janowiak, J., Mo, K.C., Ropelewski, C., Wang, J., Leetmaa, A., Reynolds, R., Jenne, R., and Joseph, D. The NCEP/NCAR 40-year reanalysis project Bull. Am. Meteorol. Soc. 77 437–71, 1996.

Kapsch, M.-L., Graversen, R.G., and Tjernström, M. Springtime atmospheric energy transport and the control of Arctic summer sea-ice extent. Nature Clim. Change, 3, 744–748, doi:10.1038/nclimate1884, 2013.

Kapsch, M.-L., Graversen, R.G., Economou, T, and Tjernström, M. The importance of spring atmospheric conditions for predictions of the Arctic summer sea ice extent. *Geophys.* Res. Lett., 41, 5288–5296, doi:10.1002/2014GL060826, 2014.

Kay, J. E., Holland, M. M., and Jahn., A. Inter-annual to multi-decadal Arctic sea ice extent trends in a warming world. *Geophysical Research Letters* 38:L15708, doi:10.1029/2011GL048008, 2011.

Koenigk, T., and Mikolajewicz, U. Seasonal to interannual climate predictability in mid and high northern latitudes in a global coupled model. *Clim. Dyn.* **32**: 783–798, doi: 10.1007/s00382-008-0419-1, 2009.

Levitus, S., Antonov, J. I., Boyer, T. P., Baranova, O. K., Garcia, H. E., Locarnini, R. A., Mishonov, A. V., Reagan, J. R., Seidov, D., Yarosh, E. S., and Zweng, M. M. World ocean heat content and thermosteric sea level change (0–2000 m), 1955–2010. Geophysical Research Letters 39(10). doi:10.1029/2012GL051106, 2012.

Lindsay, R.W., and Zhang, J. The thinning of Arctic sea ice, 1988–2003: Have we passed a tipping point? J. Clim. 18(22), 4879–4894, 2005.

Lindsay, R.W., Zhang, J., Schweiger, A.J., and Steele, M.A. Seasonal predictions of ice extent in the Arctic Ocean. J. Geophys. Res. 113, C02023, 2008.

Mahajan, S., Zhang, R., and Delworth, T.L. Impact of the Atlantic Meridional Overturning Circulation (AMOC) on Arctic Surface Air Temperature and Sea Ice Variability. J. Climate, 24, 6573–6581, https://doi.org/10.1175/2011JCLI4002.1 , 2011.

Meier, W.N., Hovelsrud, G., van Oort, B., Key, J., Kovacs, K., Michel, C., Granskog, M., Gerland, S., Perovich, D., Makshtas, A. P., and Reist, J. Arctic sea ice in transformation: A review of recent observed changes and impacts on biology and human activity, Rev. Geophys., 51,185–217, doi:10.1002/ 2013RG000431, 2014.

Meier, W.N., Fetterer, F., Savoie, M., Mallory ,S., Duerr, R., and Stroeve, J. NOAA/NSIDC Climate Data Record of Passive Microwave Sea Ice Concentration, Version 2, 1979-2011, Natl. Snow and Ice Data Cent., Boulder, Colo., doi:10.7265/N55M63M1, 2013.

Meißner, D., Klein, B., and Ionita, M. Development of a monthly to seasonal forecast framework tailored to inland waterway transport in Central Europe, Hydrol. Earth Syst. Sci. Discuss., 2017, 1-31, doi:10.5194/hess-2017-293, 2017.

Miles, M.W., Divine, D.V., Furevik, T., Jansen, E., Moros, M., and Ogilvie, A.E.J. A signal of persistent Atlantic multidecadal variability in Arctic sea ice, Geophys. Res. Lett., 41, 463–469, doi:10.1002/2013GL058084, 2014.

Notz, D., and Marotzke, J. Observations reveal external driver for Arctic sea-ice retreat. *Geophysical Research Letters* 39:L08502, doi:10.1029/2012GL051094, 2012.

Ono, J., Tatebe, H., Komuro, Y., Nodzu, M. I., and Ishii, M. Mechanisms influencing seasonal to inter-annual prediction skill of sea ice extent in the Arctic Ocean in MIROC, The Cryosphere, 12, 675-683, https://doi.org/10.5194/tc-12-675-2018, 2018.

Park, W., and Latif, M. Multidecadal and multicentennial variability of the meridional overturning circulation. Geophys. Res. Lett. 35, L22703, doi: 10.1029/2008GL035779, 2008.

Parkinson, C.L., Vinnikov, K.Y., and Cavalieri, D. J. Evaluation of the simulation of the annual cycle of Arctic and Antarctic sea ice coverages by 11 major global climate models, J. Geophys. Res., 111, C07012, doi:10.1029/2005JC003408, 2006.

Polyakov, I.V., Pnyushkov, A.V., Alkire, M.B., Ashik, I.M., Baumann, T.M. , Carmack, E.C., Goszczko, I., Guthrie, J., Ivanov, V.V., Kanzow, T., Krishfield, R., Kwok, R., Sundfjord, A., Morison, J., Rember, R., and Yulin, A. Greater role for Atlantic inflows on sea-ice loss in the Eurasian Basin of the Arctic Ocean, Science, 356 (6335), pp. 285-291 . doi: 10.1126/science.aai8204, 2017.

Schröder, D., Feltham, D. L., Flocco, D., and Tsamados M. September Arctic sea-ice minimum predicted by spring melt-pond fraction, Nat. Clim. Change., *4*, 353–357, 2014.

Schøyen H., and Bråthen, S. The Northern Sea route versus the Suez Canal: cases from bulk shipping. J. Transp. Geogr. 19, 977–983, 2011.

Screen, J.A., and Francis, J.A. Contribution of sea-ice loss to Arctic amplification is regulated by Pacific Ocean decadal variability. Nature Clim. Change 6, 856–860, 2016.

Serreze, M.C., Holland, M.M., and Stroeve, J. Perspectives on the Arctic's shrinking sea-ice cover. Science 315(5818):1533–1536, 2007.

Smith, L.C., and Stephenson, S.R. New Trans-Arctic shipping routes navigable by midcentury. Proc. Natl. Acad. Sci. U.S.A. 110*: 4871–4872, doi: 10.1073/pnas.1214212110, 2013.

5   Stroeve, J. C., Hamilton, L., Bitz, C., and Blanchard-Wigglesworth, E. Predicting September sea ice: Ensemble skill of the SEARCH sea ice outlook 2008–2013, Geophys. Res. Lett., 41(7), 2411–2418, doi:10.1002/2014GL059388, 2014.

Stroeve, J., Blanchard-Wrigglesworth, E., Guemas, V., Howell, S., Massonnet, F., and Tietsche, S. Improving predictions of Arctic sea ice extent, Eos, 96, doi:10.1029/2015EO031431, 2015.

Walsh, J.E., and Johnson, C.M. An analysis of Arctic sea ice fluctuations. J. Phys. Oceanogr. 9: 580–591, 1979.

Yu, L., Zhong, S., Winkler, J.A., Zhou, M., Lenschow, D.H., Li, B., Wang, X., and Yang, Q. Possible connections of the opposite trends in Arctic and Antarctic sea-ice cover, Nature Scientific Reports, 7, doi:10.1038/srep45804, 2017.

Zhan, Y., and Davies, R. September Arctic sea ice extent indicated by June reflected solar radiation, J. Geophys. Res. 15   Atmos., 122, 2194–2202, doi: 10.1002/2016JD025819, 2017.

Zhang, R. Mechanisms for low-frequency variability of summer Arctic sea ice extent. Proc. Natl Acad. Sci. USA **112**, 4570–4575, 2015.

25

30

35
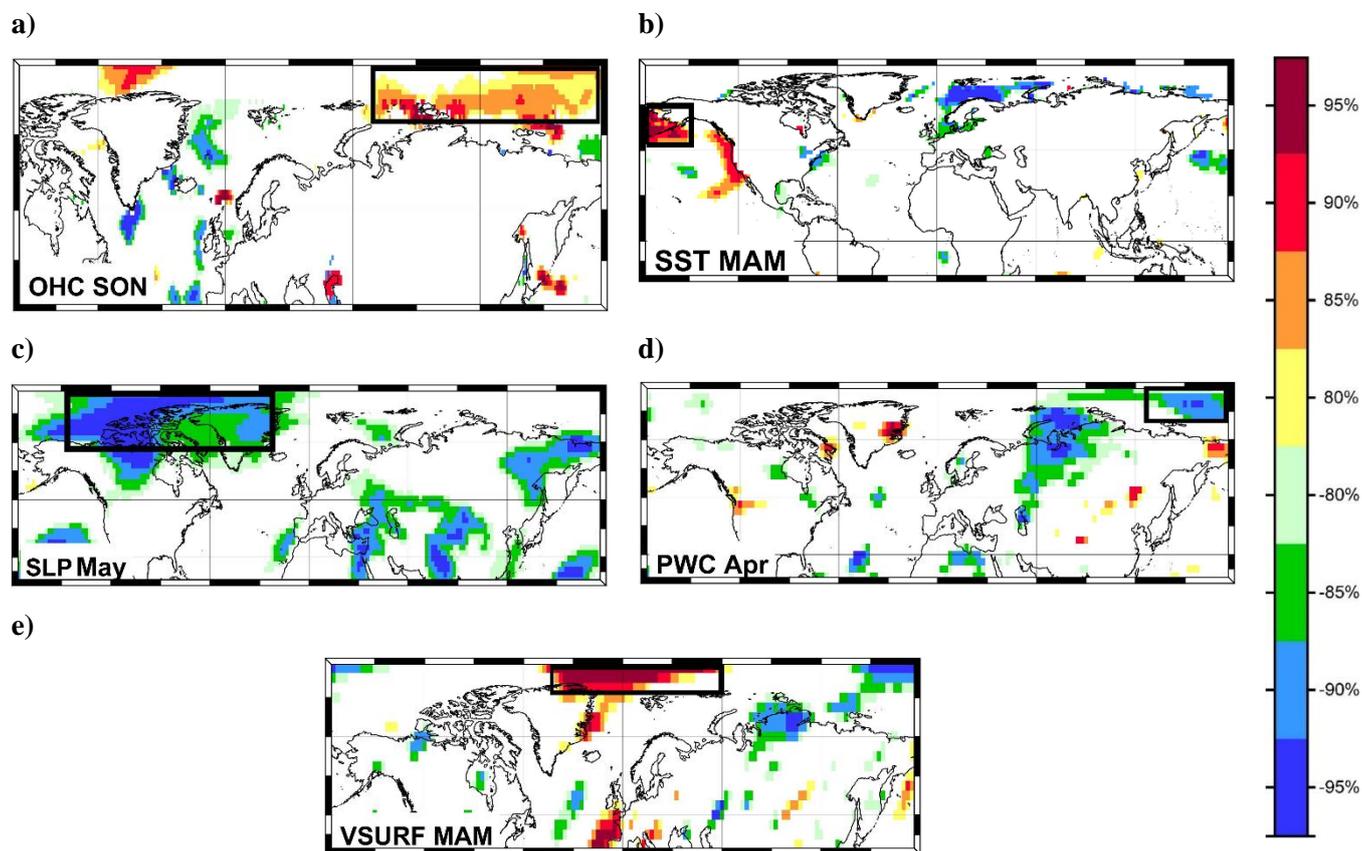
Figure 1. Stability map of the correlation between September Sea Ice Extent and a) OHC SON, b) SST MAM, c) SLP May, d) PWC Apr, and e) VSURF MAM. Regions where the correlation is stable, positive and significant for at least 80% windows are shaded with dark red (95%), red (90%), orange (85%) and yellow (80%). The corresponding regions where the correlation is stable, but negative, are shaded with dark blue (95%), blue (90%), green (85%) and light green (80%). The black boxes indicate the regions used for the September sea ice extent at the end of May.

a)
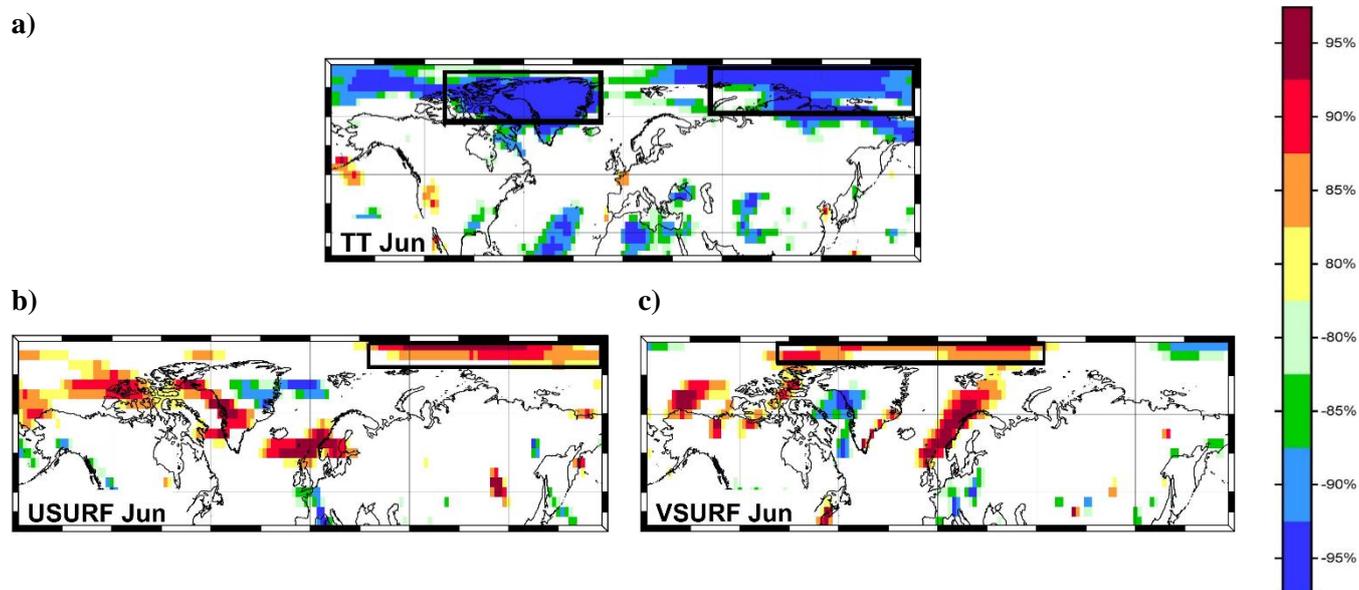
Figure 2. Stability map of the correlation between September Sea Ice Extent and a) TT Jun, b) USURF Jun and c) VSURF Jun. Regions where the correlation is stable, positive and significant for at least 80% windows are shaded with dark red (95%), red (90%), orange (85%) and yellow (80%). The corresponding regions where the correlation is stable, but negative, are shaded with dark blue (95%), blue (90%), green (85%) and light green (80%). The black boxes indicate the regions used for the September sea ice extent at the end of June.
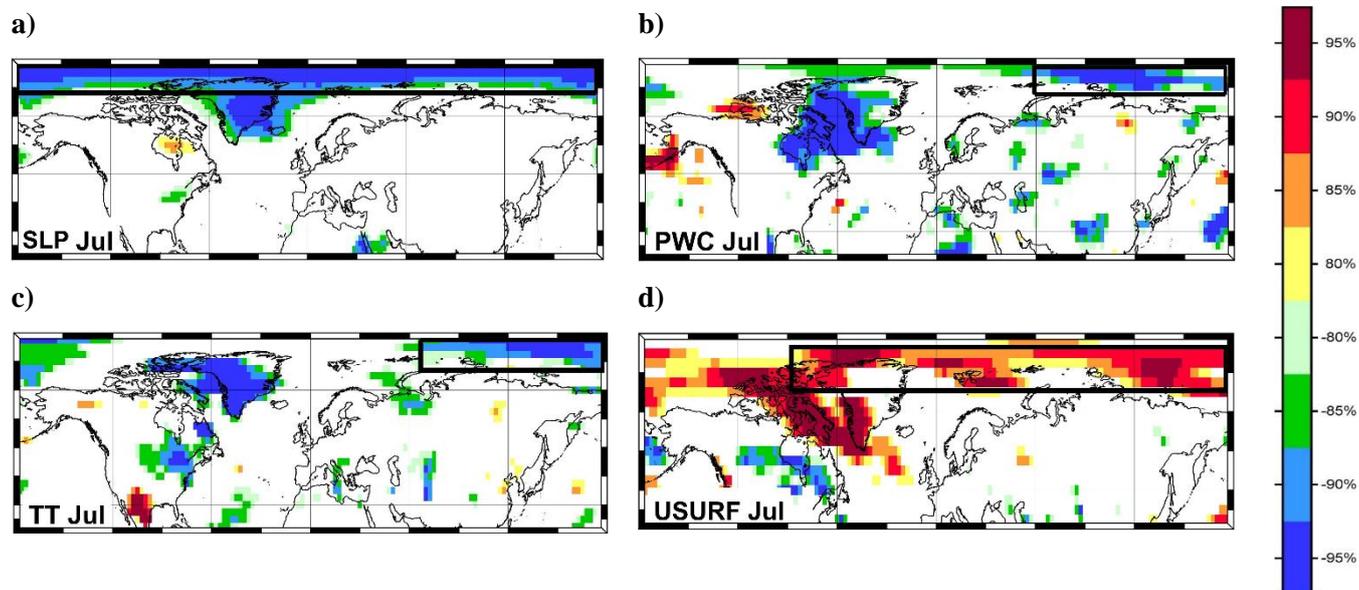
Figure 3. Stability map of the correlation between September Sea Ice Extent and a) SLP Jul, b) PWC Jul, c) TT Jul and d) USURF Jul. Regions where the correlation is stable, positive and significant for at least 80% windows are shaded with dark red (95%), red (90%), orange (85%) and yellow (80%). The corresponding regions where the correlation is stable, but negative, are shaded with dark blue (95%), blue (90%), green (85%) and light green (80%). The black boxes indicate the regions used for the September sea ice extent at the end of July.
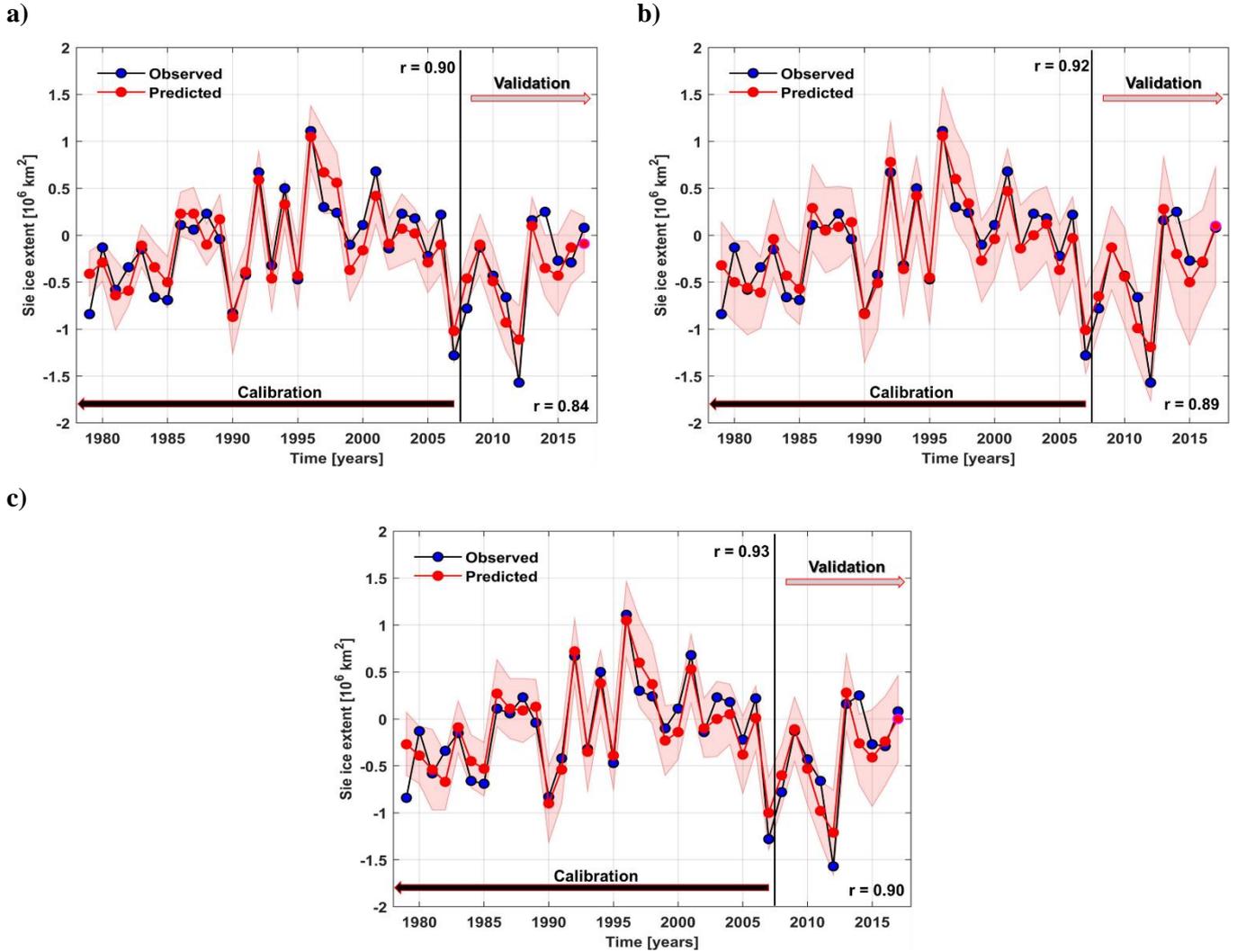
Figure 4. Observed (black) and predicted (red) September Sea Ice Extent detrended anomalies over the period 1979-2017 based on a) May, b) June and c) July predictors from the stable regions. The shaded area represents the 95% uncertainty bounds.

a)

b)

c)
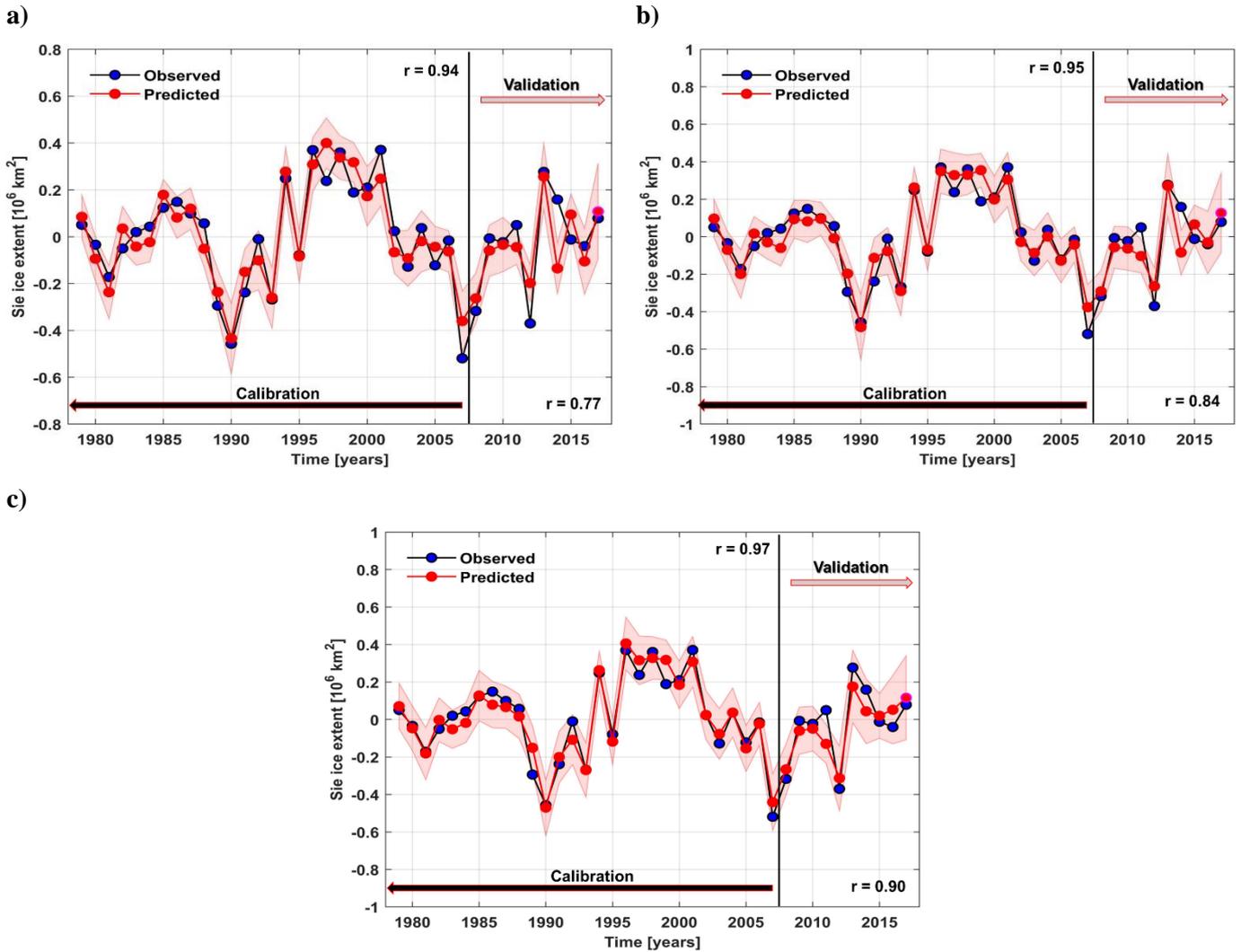
Figure 5. Observed (black) and predicted (red) East Siberian Sea Ice Extent detrended anomalies over the period 1979-2017 based on a) May, b) June and c) July predictors from the stable regions. The shaded area represents the 95% uncertainty bounds.

Table 1. Variables retained for the September pan-Arctic sea ice extent forecast (black boxes in Figure 1, 2 and 3). Seasonal averages are indicated as spring MAM and autumn SON; single months are abbreviated with the first three letters of the month.

	May Data	**June Data**	**July Data**
Persistence	SIE Mar	SIE Mar	SIE Mar
Ocean variables	OHC SON	OHC SON	OHC SON
	SST MAM	SST MAM	SST MAM
	AMO – L4	AMO – L4	AMO – L4
Atmospheric variables	SLP May	SLP May	SLP May, Jul
	VSURF MAM	VSURF MAM, Jun	VSURF MAM, Jun
	PWC Apr	PWC Apr	PWC April, Jul
		USURF Jun	USURF Jun, Jul
		TT Jun	TT Jun, Jul

Table 2. The correlation coefficients between the detrended pan-Arctic September sea ice extent and the regional September sea ice extent

	Lag 4	Lag 3	Lag 2	Lag 1	Lag 0
Baffin	0.07	0.09	0.34	0.40	0.39
Barents	0.20	0.16	0.27	0.13	0.14
Beaufort	0.15	0.24	0.37	0.51	**0.60**
Bering	-0.30	-0.02	0.14	0.00	-0.04
Canadian	0.07	-0.16	0.01	0.52	0.49
Chukchi	-0.26	0.03	0.09	0.53	**0.60**
East Siberian	0.19	0.24	0.39	0.61	**0.72**
Greenland	0.04	0.06	0.22	0.16	-0.07
Hudson	0.44	0.51	0.46	0.38	0.47
Kara	0.09	-0.03	0.05	-0.08	-0.07
Laptev	0.34	0.32	0.40	0.37	0.53

Table 3. Variables retained for the September East Siberian sea ice extent forecast (black boxes in Figure S2, S3 and S4). Seasonal averages are indicated as spring MAM; single months are abbreviated with the first three letters of the month.

	May Data	**June Data**	**July Data**
Persistence		SIE Jun	SIE Jun, Jul
Ocean variables	OT100 – L4, L1	OT100 – L4, L1	OT100 – L4, L1
	SST MAM	SST MAM,	SST MAM
Atmospheric variables	SLP Jan	SLP Jan	SLP Jan
	VSURF MAM	VSURF MAM	VSURF MAM, Jul
	PWC May	PWC May	PWC May, Jul
	TT May	TT May, Jun	TT May, Jun, Jul
	DW MAM	DW MAM	DW MAM